

# Prediction of Developmental Changes due to Climate Change in ‘Delaware’ Grapes in Osaka, Japan, based on Simulated Data

Masahiro KAMIMORI\* and Kazuya HIRAMATSU

Local Independent Administrative Agency, Research Institute of Environment, Agriculture and Fisheries, Habikino, Japan

## Abstract

We predicted developmental changes (endodormancy breaking, budding, and full-flowering) in ‘Delaware’ grapes induced by climate change in Osaka Prefecture, Japan, to consider adaptation measures. Endodormancy breaking (the day when the accumulation of chilling hours below 7.2°C reached 600 h; DCH600), budding, and full-flowering dates were estimated using models based on air temperature. A projected air temperature dataset until 2100 with 1 km resolution for two emission scenarios of Representative Concentration Pathways (RCP2.6, low; RCP8.5, high) was applied to these models. DCH600 was delayed by 19 (RCP2.6) and 21 (RCP8.5) days in 2041/2042-2050/2051, whereas in 2091/2092-2099/2100, it was projected to be 21 (RCP2.6) and 48 (RCP8.5) days later than that in 1981/1982-1990/1991. Conversely, the budding date was earlier by 6 (RCP2.6) and 7 (RCP8.5) days in 2041-2050 than in 1981-1990. The full-flowering date was earlier by 9 (RCP2.6) and 12 (RCP8.5) days in 2041-2050 than in 1981-1990. Based on these prediction results, it may be possible to sustain ‘Delaware’ grape production until 2050 through advanced cultivation management. However, after 2050 under RCP8.5, delayed DCH600 and inadequate chilling are predicted, necessitating a change in cropping type or conversion to other fruit trees.

**Discipline:** Horticulture

**Additional key words:** budding date, chilling hours, endodormancy breaking, full-flowering date, table grapes

## Introduction

Perennial crops have narrower climate adaptability than annual crops (Sugiura et al. 2009). Hence, fruit industry, such as grapes production, is considered to be particularly vulnerable to climate change (Ministry of Agriculture, Forestry and Fisheries 2021). Ongoing climate change has already had a profound impact on grapes; for example, developmental changes and poor skin color, have been reported previously (Sugiura et al. 2012). As air temperatures are expected to continue to increase, these challenges will become more serious. Hence, there is an urgent need for sustainable grape production to develop adaptation plans for climate change by quantitatively predicting future changes in grape cultivation. However, such prediction needs a model that links development in grapes with air temperature. To date, studies have been conducted only for a few cultivars (Mosedale et al. 2016, Sugiura et al. 2019), and there is no

study on ‘Delaware’ grape.

‘Delaware’ grape (*Vitis labruscana* Bailey) is a table grape cultivar that has the third largest growing area in Japan. Moreover, in Osaka Prefecture in the Kansai region of Japan, ‘Delaware’ is the main cultivar that accounts for 80% (266.7 ha) of grape production (Ministry of Agriculture, Forestry and Fisheries 2018). We previously confirmed that ‘Delaware’ grape, under open field conditions in Osaka, showed accelerations in budding and full-flowering from 1963 to 2010 (Kamimori et al. 2019) and statistically modeled the relationships between the budding and full-flowering dates and air temperature using data collected over nearly 50 years (Kamimori et al. 2020). The budding and full-flowering dates are indicators of the timing of cultivation management practices, such as pest control, shoot treatment, and gibberellic acid application. Grape growers combine different cropping types or varieties to shift the budding and full-flowering date, when cultivation management

---

\*Corresponding author: KamimoriM@mbox.kannousuiken-osaka.or.jp  
Received 9 November 2021; accepted 20 January 2022.

practices are concentrated, and disperse during the busy season. In fruit cultivation, it is more difficult to change cropping type or replant than in annual crop cultivation; therefore, changing cropping types or varieties to adapt to climate change must be considered more than 10 years in advance. Hence, predicting future developmental changes in ‘Delaware’ is important to formulate long-term cultural practices. Furthermore, the endodormancy breaking of grapes requires accumulation of chilling hours below 7.2°C (Magoon & Dix 1943), and inadequate chilling due to warm autumn and winter causes abnormal (decreased, delayed, and non-uniform) budding in heated cultivation in Japan (Hirose et al. 2000, Osada & Ohe. 2010, Sugiura et al. 2009). Hence, the accumulation of chilling hours below 7.2°C is an important indicator of the heating timing in the heated cultivation of table grapes. Although chilling hours below 7.2°C are expected to decrease because of climate change, studies on the prediction of future changes in chilling hours using projected air temperature are limited.

In this study, we predicted future developmental changes (endodormancy breaking, budding, and full-flowering) in ‘Delaware’ grapes in Osaka using the projected air temperatures in global warming scenarios. Furthermore, the geographical distribution of the developmental change in ‘Delaware’ was mapped to visualize the impact of climate change in Osaka. Based on these prediction results, the impact of climate change on future ‘Delaware’ grape production and adaptation plans are discussed, using Osaka as the model region.

## Materials and methods

### 1. Study area

The areas for the study were retrieved from a gridded dataset, called the National Land Numerical Information Land Utilization Tertiary Mesh Data (2016) (Ministry of Land Infrastructure, Transport and Tourism <<https://nlftp.mlit.go.jp/ksj/index.html>>. Accessed on 1 November 2020). The spatial resolution of the dataset was 1 km (each grid cell measured 45" longitude × 30" latitude). We selected grid cells containing “other farming land” (except for paddy fields; 216 grids) in the major ‘Delaware’ grape production regions in Osaka (Chubu [Moriguchi, Hirakata, Yao, Neyagawa, Daito, Kashiwara, Kadoma, Higashiosaka, Shijonawate, and Katano City] and Minamikawachi [Tondabayashi, Kawachinagano, Matsubara, Habikino, Fujiidera, and Osakasayama City, Taishi Town, Kanan Town, and Chiharaakasaka Village]) (Fig. 1).

### 2. Climate data

The actual air temperature (daily mean, maximum, and minimum) of each grid cell was obtained using the Agro-Meteorological Grid Square Data (AMGSD) system operated by the National Agricultural Research Organization, Japan, which is a 1 km resolution climate dataset (each grid cell measures 45" longitude × 30" latitude), estimated using statistics from meteorological observation stations of the Japan Meteorological Agency (JMA) (Ohno et al. 2016). The projected air temperatures

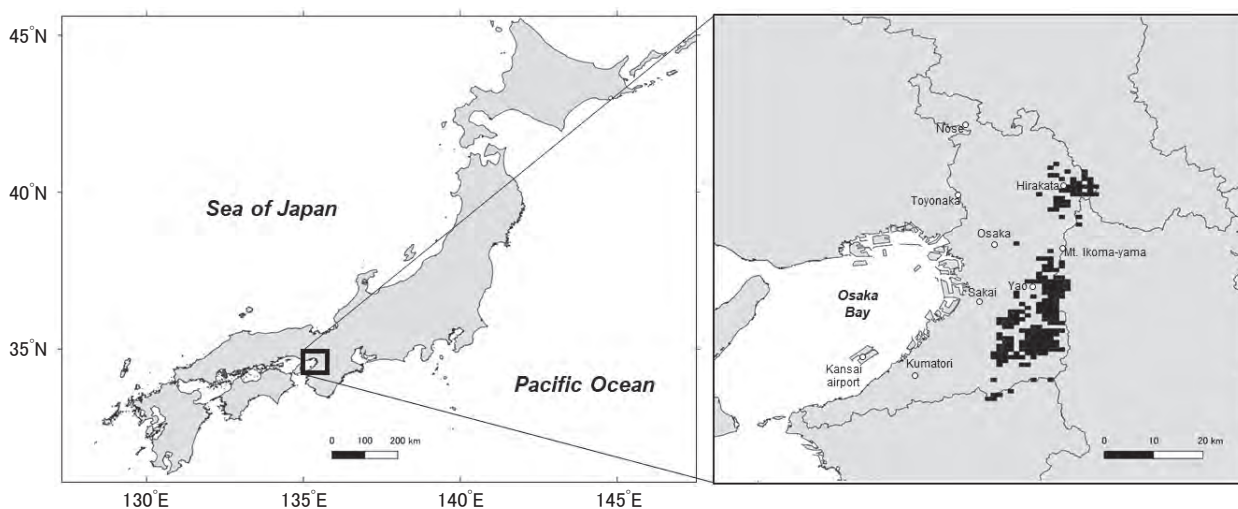


**Fig. 1. Map of Japan and Osaka Prefecture**

Shaded area denotes the study areas (grid cells containing “other farming lands” [except for paddy fields] in the major ‘Delaware’ grape production area). The white circle denotes the Automated Meteorological Data Acquisition System observatories.

of each grid cell were obtained from the AMGSD dataset using climate change scenarios derived from global climate models (GCMs) with a 1 km resolution spanning the period 1981-2100 (Nishimori et al. 2019). In this study, we used daily mean air temperature, daily maximum air temperature, and daily minimum air temperature calculated using five GCMs (MIROC5, MRI-CGCM3, GFDL-CM3, CSIRO-Mk3-6-0, and HadGEM2-ES) simulated for two emission scenarios of Representative Concentration Pathways (RCP2.6, a very low greenhouse gas emission scenario and RCP8.5, a very high greenhouse gas emission scenario) in the AMGSD dataset. As HadGEM2-ES under the RCP8.5 scenario did not provide the projected air temperatures in 2100, we used the projected air temperatures until 2099. We obtained the actual air temperature and projected air temperature of each grid cell in the study area.

In the simulation described in subsection 3 (chilling hour), we used the actual air temperatures from October 1981 to March 2021 and the projected air temperatures from October 2021 to March 2100. In the simulation described in subsection 4 (budding and full-flowering dates), we used the actual air temperatures from February to June during 1981-2020 and the projected air temperatures from February to June of 2021-2050.

### 3. Estimation of chilling hour below 7.2°C

In this study, we investigated the day when the accumulation of chilling hours below 7.2°C reached 600 h (DCH600) because a previous study showed that endodormancy breaking in 'Delaware' grape occurs when chilling hours below 7.2°C exceed 600 h (Hirose et al. 2000). DCH600 was estimated using the method of Seino et al. (1981) to estimate the chilling hours below 7.2°C per day from the daily maximum air temperature ( $T_{max}$ , °C) and daily minimum air temperature ( $T_{min}$ , °C) according to Eq. 1.

$$D_L = \frac{48}{\pi} \sin^{-1} \left[ \sqrt[3]{\frac{-q + \sqrt{p}}{2}} + \sqrt[3]{\frac{-q - \sqrt{p}}{2}} - \frac{1}{3} \right] \quad [1]$$

$$p = q^2 + 0.0439 \quad q = a - 0.2593 \quad a = -\frac{3L}{K}$$

$$L = T_s - T_{min} \quad (T_{min} \leq T_s < T_{max}) \quad K = T_{max} - T_{min}$$

where  $T_s$  (°C) is the specific temperature (in this case, 7.2°C) and  $D_L$  is the chilling hours below 7.2°C per day (h). In the case of  $T_{min} > 7.2^\circ\text{C}$ ,  $D_L$  is 0 h. In the case of  $T_{max} \leq 7.2^\circ\text{C}$ ,  $D_L$  is 24 h. The calculation starting date was October 1, and the end date was March 31 of the following year. In addition, this estimation method

must be corrected based on the distance to the coast. Therefore, we examined the relationship between the estimated  $D_L$  and distance to the coast in Osaka using the method described by Seino et al. (1981). Temperature data at 60 min intervals were obtained from the Automated Meteorological Data Acquisition System (AMeDAS) observatories located in Osaka (Fig. 1) over three seasons (from 2018/2019-2020/2021), and hourly-based  $D_L$  were calculated. The daily maximum air temperature and daily minimum air temperature were also acquired from the AMeDAS observatories, and the estimated  $D_L$  was calculated using Eq. 1. We analyzed the relationship between the ratio of the hourly-based  $D_L$  to the estimated  $D_L$  ( $F$  value) and the distance to the coast of AMeDAS observatories (Fig. 2) and obtained Eq. 2.

$$F = 0.958 + 0.0055 \times R \quad [2]$$

where  $R$  is the distance from the coast to the grid cells. We performed a correction calculation of  $D_L$  based on the distance to the coast according to Eq. 2. The applicability of Eq. 2 was verified using the data over seven seasons (from 2011/2012 to 2017/2018) from the AMeDAS observatories, and the estimated DCH600 agreed well with the hourly-based DCH600 (Table 1). However, among the AMeDAS observatories, the  $F$  value of Osaka City was excluded from the regression equation because no consistent trend was found in the relationship between the  $F$  values and the distance to the coast. We calculated

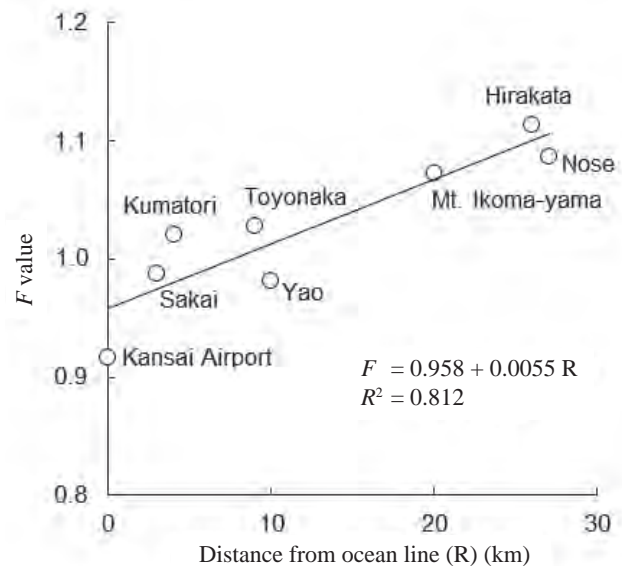


**Fig. 2. Relationship between  $F$  value (the ratio of the hourly-based chilling hours to the estimated chilling hours) and distance from the coastline ( $R$ ) of the Automated Meteorological Data Acquisition System observatories in the data of three seasons (2018/2019-2020/2021)**

the distance from the coast to each grid cell using the Quantum Geographic Information System (QGIS) version.3.14.16 (QGIS Developer Team, <http://www.qgis.org/>). We corrected the estimated  $D_L$  of each grid cell by multiplying the  $F$  value. When the estimated  $D_L$  exceeded 24 h after multiplying the  $F$  value, the estimated  $D_L$  was 24 h. When the accumulated value of estimated  $D_L$  within the period (from October 1 to March 31 in the next year) did not reach 600 h, we recorded the grid cells as “No reach.” The data with “No reach” were excluded from the calculation of the estimated DCH600.

**4. Models to estimate budding and full-flowering dates**

Data on the budding and full-flowering dates of the ‘Delaware’ grape grown under open-field conditions obtained from the Research Institute of Environment, Agriculture and Fisheries, Osaka Prefecture (located at 34°32’ N, 135°35’ E, and 70 m altitude) from 1963 to 2019 (except from 2011 to 2017) were analyzed. The soil type in the field was fine-textured terrace yellow soil. We selected three to four ‘Delaware’ grapevines ( $\geq 5$  years old) trained on a horizontal trellis with long cane pruning for observation. The budding date was defined as the date when the buds were swollen, and more than 80% of all buds were exposed from the scale. The full-flowering date was defined as the date when more than 80% of all florets were open in more than 80% of all flower clusters without gibberellic acid application. In predicting budding and full-flowering dates, we used the model of developmental index (DVI) by Nakagawa and Horie (1995). The DVI value is calculated by summing the daily development rate (DVR):

$$DVI_n = \sum_{i=1}^n DVR_i$$

where  $DVI_n$  is the DVI on day  $n$  and  $DVR_i$  is the DVR on the  $i$ -th day from the starting date. For predicting the budding date, the DVI of the starting date (February 21) was defined as 0, and the budding date was defined as the date when DVI first exceeded 1. Furthermore, the starting date was determined as follows: we set starting dates between January 1 to March 13 with step increases of 5-10 days, and the starting date (February 21) yielding the lowest root mean square error (RMSE) was adopted. For predicting the flowering date, DVI of the starting date (the day after budding) was defined as 0, and the full-flowering date was defined as the date when DVI first exceeded 1. Daily DVR was calculated as a function of daily mean temperature ( $T_{mea}$ , °C) using the following DVR models (Kamimori et al. 2020):

$$Budding\ date\ DVR = \frac{1}{G_1} \times \frac{1}{1 + \exp\{-A_1(T_{mea} - T_{h1})\}} \quad [3]$$

$$Full-flowering\ date\ DVR = \frac{1}{TU}(T_{mea} - T_b) \quad [4]$$

where  $G_1$ ,  $A_1$ ,  $T_{h1}$ ,  $TU$ , and  $T_b$  are the parameters (Table 2). Based on the prediction results of endodormancy breaking, chilling hours would be inadequate in the future. The budding prediction model does not consider inadequate chilling and cannot be used in such situations. Thus, in the simulation of budding and full-flowering dates, we simulated until the year 2050, when endodormancy

**Table 1. Comparisons between the hourly-based DCH600 (the day when the accumulation of chilling hours below 7.2°C reached 600 h) and estimated DCH600 at the Automated Meteorological Data Acquisition System (AMeDAS) observatories for 2011/2012-2017/2018**

AMeDAS observatories	Latitude	Longitude	Distance from ocean line (km)	$F^z$	Hourly based DCH600 <sub>MEAN</sub> <sup>y</sup>	Hourly based DCH600 <sub>STD</sub> <sup>x</sup>	RMSE <sup>w</sup> (days)
Nose	34°56’ N	135°27’ E	27	1.086	December 22	7.1	0.5
Toyonaka	34°47’ N	135°26’ E	9	1.028	January 7	8.5	2.3
Hirakata	34°48’ N	135°40’ E	26	1.114	January 6	8.6	1.2
Osaka	34°40’ N	135°31’ E	7	0.890	January 16	10.7	-
Mt. Ikoma-yama	34°40’ N	135°40’ E	20	1.073	December 18	6.4	1.6
Yao	34°35’ N	135°36’ E	10	0.982	January 10	8.9	1.5
Sakai	34°33’ N	135°29’ E	3	0.987	January 14	10.4	2.6
Kumatori	34°23’ N	135°21’ E	4	1.020	January 9	8.8	2.9
Kansai Airport	34°26’ N	135°13’ E	0	0.917	January 27	13.8	3.4

<sup>z</sup>  $F$  is the ratio of the hourly based  $D_L$  to the estimated  $D_L$  over three seasons (2018/2019-2020/2021).

<sup>y</sup> Mean value of seven seasons (2011/2012-2017/2018) of hourly based DCH600

<sup>x</sup> Standard Deviation value of seven seasons (2011/2012-2017/2018) of hourly based DCH600

<sup>w</sup> Root Mean Square Error (RMSE) value of seven seasons (2011/2012-2017/2018) of DCH600 between the hourly based DCH600 and estimated DCH600 corrected by the developed equation from the data of three seasons (2018/2019-2020/2021) (see Fig. 2)

**Table 2. Parameters for developmental rate (DVR) models**

Developmental stage	Starting date	Parameter					RMSE <sup>z</sup> (days)
		A <sub>1</sub> (°C <sup>-1</sup> )	T <sub>h1</sub> (°C)	G <sub>1</sub> (days)	TU (°C·day)	T <sub>b</sub> (°C)	
Budding	February 21	0.1	53.5	0.5	-	-	2.4
Full-flowering	The day after budding	-	-	-	414.9	7.4	2.1

<sup>z</sup> Root mean square error (RMSE) values between the observation date and predicted date in 1963-2001

breaking is expected to occur by February 21, the starting date of the budding prediction model.

### 5. Simulation of the geographical distribution of developmental changes in ‘Delaware’ grapes in Osaka

The DCH600 values from 1981/1982-1990/1991, 2011/2012-2020/2021, and 2041/2042-2050/2051 were simulated for all grid cells for each GCM, and the five values obtained were averaged for each year range and mapped using QGIS. The budding and full-flowering dates in 1981-1990, 2011-2020, and 2041-2050 were simulated in all grid cells for each GCM, and the five values obtained were averaged for each year range and mapped using QGIS.

## Results and discussion

### 1. Climate data

The decadal mean air temperatures in the study areas from 1981-1990 to 2091-2100 are shown in Figure 3. These values increased gradually and were higher by 2.4°C (RCP2.6) and 2.8°C (RCP8.5) in 2041-2050 than in 1981-1990. The standard deviations (SDs) between GCMs were 0.76°C and 0.68°C, respectively. The difference owing to the different emission scenarios increased after approximately 2050, and the average temperature in 2091-2100 was 2.2°C (RCP2.6) and 5.6°C (RCP8.5) higher than that in 1981-1990. The SDs between GCMs were 0.56°C and 1.05°C, respectively. A similar increase in air temperature has been reported in other studies in Japan (Ishigooka et al. 2017, Sugiura et al. 2019).

### 2. Estimated DCH600

The changes in the DCH600 in the study areas are shown in Figure 4. This date gradually delayed, and the 10-year average DCH600 was delayed by 19 days (RCP2.6) and 21 days (RCP8.5) in 2041/2042-2050/2051 than in 1981/1982-1990/1991. The SDs between GCMs were 7.2 and 6.7 days, respectively. The difference owing to the different emission scenarios increased after approximately 2050/2051, and the average DCH600 in 2091/2092-2099/2100 was 21 days (RCP2.6) and

48 days (RCP8.5) later than in 1981/1982-1990/1991. The SDs between GCMs were 6.7 and 7.9 days, respectively. In RCP2.6, DCH600 stabilized at approximately 105 (mid-January) after 2050/2051. Alternatively, in RCP8.5, DCH600 continued to be delayed, reaching approximately 135 (mid-February) by 2100. In this case, the endodormancy breaking would be inadequate at the current heating timing in Osaka (mid-January to late-January); as a result, abnormal budding could be caused. Therefore, it is necessary to delay the heating timing, and the benefits of the advance of the development and harvesting time of ‘Delaware’ grape via heated cultivation cannot be expected.

The ratio of grid cells for which the chilling hours below 7.2°C did not reach 600 h within the calculation period (from October 1 to March 31 in the next year) in the study areas are also shown in Figure 4. The difference

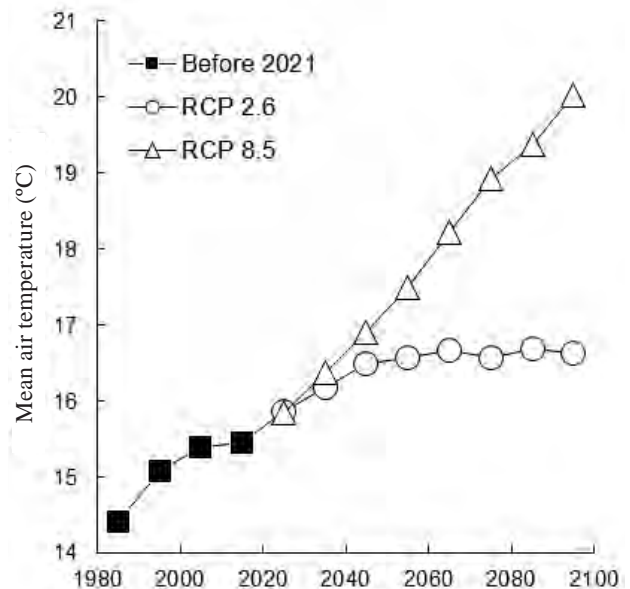


**Fig. 3. Decadal mean air temperatures averaged 216 grid cells (“other farming lands” in the major ‘Delaware’ grape production area)**

The graph was based on actual air temperatures from 1981 to 2020 and projected air temperatures in 2021-2100. The projected air temperatures were averaged over five global climate models (GCMs) and are shown for each emission scenario (RCP).

owing to the different emission scenarios increased after 2061/2062, with the number from 2061/2062-2070/2071 being 0.2 grid cells (0.1%) in RCP2.6 and 16.0 grid cells (7.4%) in RCP8.5. The SDs between GCMs were 0.3 grid cells and 19.9 grid cells, respectively. The average values in 2091/2092-2099/2100 were 0.1 grid cells (0.04%) in RCP2.6 and 95.4 grid cells (43.9%) in RCP8.5. The SDs between GCMs were 0.1 grid cells and 70.1 grid cells, respectively. Although the differences between GCMs were large, there were many grid cells in which chilling hours below 7.2°C did not reach 600 h after 2061/2062 in RCP8.5. This suggests that there is a risk of abnormal budding because of inadequate chilling, even in unheated cultivation and open-field cultivation.

### 3. Estimated budding and full-flowering dates

The changes in budding dates in the study areas are shown in Figure 5. This date gradually advanced, and the 10-year average budding date was earlier by 4 days (both RCP2.6 and RCP8.5) in 2021-2030 than in 1981-1990. The SDs between GCMs were 1.0 and 2.5 days, respectively. The average budding date in 2041-2050 was 6 days (RCP2.6) and 7 days (RCP8.5) earlier than that in 1981-1990. The SDs between GCMs were 3.0 and 1.8 days, respectively. The changes in the full-flowering date in the study areas are shown in Figure 6.

This date gradually advanced, and the 10-year average full-flowering date was earlier by 7 days (both RCP2.6 and RCP8.5) in 2021-2030 than in 1981-1990. The SDs between GCMs were 2.6 and 2.8 days, respectively. The average full-flowering date in 2041-2050 was 9 days (RCP2.6) and 12 days (RCP8.5) earlier than that in 1981-1990. The SDs between GCMs were 3.0, and 3.3 days, respectively.

Among the environmental factors, budding and full-flowering dates are primarily influenced by air temperature (Kamimori et al. 2020). The budding and full-flowering dates of ‘Delaware’ grape were predicted to advance by 2050 as the temperature increased (Figs. 5 and 6). This is consistent with the prediction of full-flowering dates in ‘Kyoho’ grape (Sugiura et al. 2019). ‘Delaware’ growers in Osaka are puzzled by accelerations of budding and full-flowering to date (Kamimori et al. 2019) because conventional experiential timing of cultivation management practices cannot be applied, the results suggest that these accelerations continue further into 2050. Furthermore, although the budding and full-flowering dates in open-field cultivation were predicted to advance, DCH600 (heating timing in heated cultivation) was predicted to delay as described above, possibly making it difficult to distribute labor among different cropping types. However, in the case of the

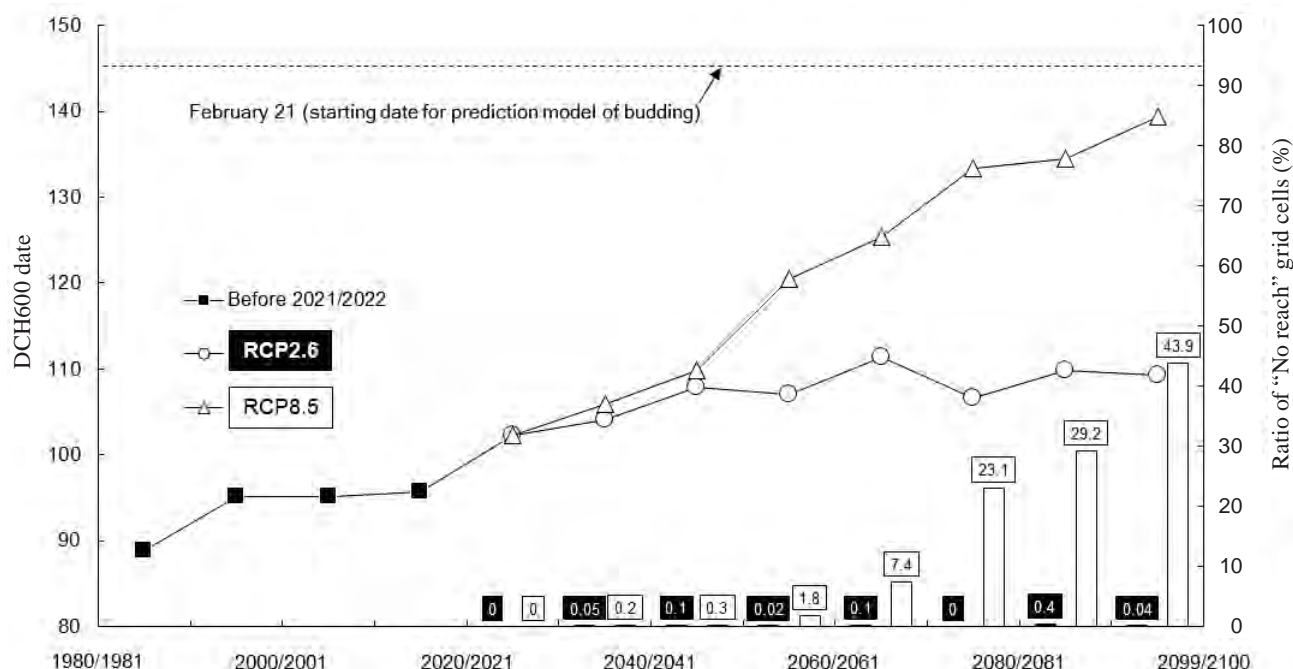


Fig. 4. Decadal estimated DCH600 and ratio of “No reach” grid cells averaged 216 grid cells (“other farming lands” in the major ‘Delaware’ grape production area)

DCH600, the number of days from October 1. The graph was based on actual air temperatures in 1981/1982-2020/2021 and projected air temperatures in 2021/2022-2099/2100. The estimated values from projected air temperatures were averaged over five global climate models (GCMs) and are shown for each emission scenario (RCP). 2091/2092-2099/2100 was the average of nine seasons. The data with “No reach” were excluded from the calculation of the estimated DCH600.

accelerations of budding and full-flowering date and the delay of DCH600 predicted by 2050 in this study, such challenges would not occur until at least 2050.

**4. Geographical distribution of the developmental changes in 'Delaware' grapes**

The geographical distribution of DCH600 in the study areas are shown in Figure 7. In 1981/1982-1990/1991, the percentage of grid cells at 84-91 (the number of days from October 1) was the highest at 47.7% (103 grid cells). However, in 2041/2042-2050/2051, the percentages of grid cells at 105-112 and 112-119 were 35.6% (77 grid cells) and 27.8% (60 grid cells), respectively, in RCP2.6. The percentages of grid cells at 105-112 and 112-119 were 31.9% (69 grid cells) and 33.3% (72 grid cells), respectively, in RCP8.5. The geographical distribution of the budding date of 'Delaware' grapes in the study areas is shown in Figure 8. In 1981-1990, the percentage of grid cells at 97-100 day of the year (DOY) was the highest at 61.1% (132 grid cells). However, in 2041-2050, the percentage of grid cells at 91-94 DOY was the highest at 52.8% (114 grid cells) in RCP2.6 and 64.4% (139 grid cells) in RCP8.5. The geographical distribution of the full-flowering date of 'Delaware' grapes in the study areas is shown in Figure 9. In 1981-1990, the percentage of grid cells at 146-150 DOY was the highest at 53.7%

(116 grid cells). However, in 2041-2050, the percentage of grid cells was the highest at 138-142 DOY at 49.0% (106 grid cells) in RCP2.6, and at 134-138 DOY at 58.3% (126 grid cells) in RCP8.5.

Osaka Prefecture is surrounded by the Osaka Bay and three mountain ranges (Hokusetsu, Kongo Ikoma, and Izumi Katsuragi) and belongs to the Seto Inland Sea climate, which is warm and dry throughout the year, making it ideal for grape production. The temperature distribution in Osaka is characterized by high temperatures in the plains and low temperatures closer to mountainous areas. The characteristics of this temperature distribution and the trend of 'Delaware' grape development were almost identical, with DCH600 tending to be later in the plains and earlier closer to mountainous areas (Fig. 7). Similarly, budding and full-flowering dates were earlier in the plains and later closer to mountainous areas (Figs. 8 and 9). Similar trends were observed in both RCP2.6 and RCP8.5; however, the 2040s under RCP8.5 showed a slightly wider range of delay in DCH600 and accelerations in budding and full-flowering mainly in the plains than those under RCP2.6. It was shown that the timing of adopting adaptation measures differs depending on the region and the emission scenarios.

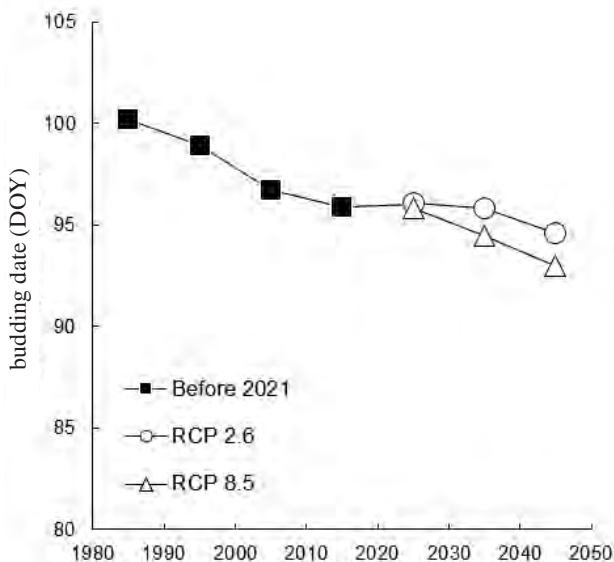


**Fig. 5. Decadal estimated budding dates of 'Delaware' grape averaged 216 grid cells ("other farming lands" in the major 'Delaware' grape production area)**  
DOY, the number of days from January 1. The graph was based on actual air temperatures in 1981-2020 and projected air temperatures in 2021-2100. The estimated values from projected air temperatures were averaged over five global climate models (GCMs) and are shown for each emission scenario (RCP).

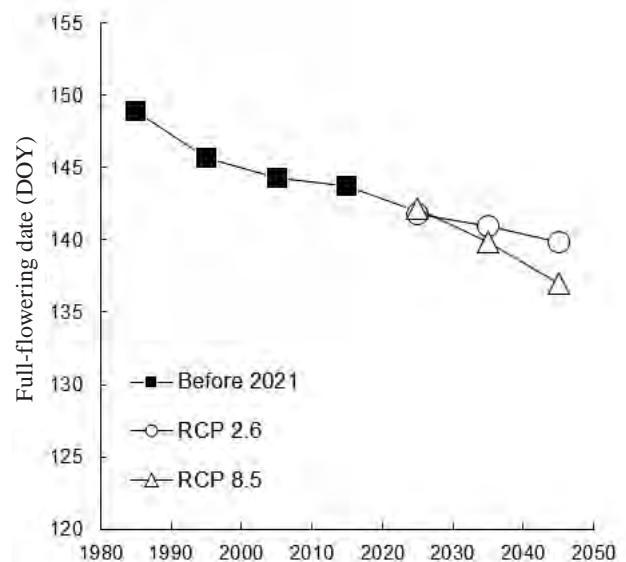


**Fig. 6. Decadal estimated full-flowering dates of 'Delaware' grape averaged 216 grid cells ("other farming lands" in the major 'Delaware' grape production area)**  
DOY, the number of days from January 1. The graph was based on actual air temperatures in 1981-2020 and projected air temperatures in 2021-2100. The estimated values from projected air temperatures were averaged over five global climate models (GCMs) and are shown for each emission scenario (RCP).

### 5. Adaptation measures

In the future, abnormal budding in heated cultivation with the current heating timing in Osaka (mid to late January) is expected to occur due to delayed endodormancy breaking. To cope with such delayed endodormancy breaking, it is necessary to start heating after confirming endodormancy breaking by air temperature observation data. AMGSD can be used to visualize the endodormancy breaking timing in ‘Delaware’ grape production areas in Osaka and help growers to determine the heating timing. Moreover, AMGSD provides temperature forecast values from “today” (the day of AMGSD use) up to 26 days after “today” based on numerical forecasts by JMA (Ohno et al. 2016). We can grasp the endodormancy breaking timing with high accuracy in advance using this forecast data. Adaptation measures for inadequate chilling include cyanamide (Kuroi 1985) and high-temperature treatment (Togano et al. 2016). Cyanamide is widely used to accelerate endodormancy breaking and to prevent abnormal budding in heated cultivation in Japan. High-temperature treatment (maintaining the temperature inside the greenhouse at 35°C to 40°C) is extended in Shimane Prefecture and can be used with cyanamide

treatment. In future heated cultivation, the efficient use of these treatments for endodormancy breaking is required. Moreover, treatments for endodormancy breaking may be useful in unheated cultivation and open-field cultivation when inadequate chilling occurs. Furthermore, low-chilling table grape cultivars must be evaluated or bred to prepare for inadequate chilling hours in ‘Delaware’ grapes, similar to the evaluation of low-chilling ‘Okinawa’ in peach (Matsumoto et al. 2019).

To cope with annual variations in budding and full-flowering dates, we developed models to predict the budding and full-flowering dates of ‘Delaware’ grapes based on daily mean temperature (Kamimori et al. 2020). These models allow us to predict the current year’s budding and full-flowering dates, and it is possible to manage culture practices according to year-to-year variations. Furthermore, temperature forecast values by AMGSD can be used to predict budding and full-flowering dates with high accuracy. In future studies, a model that can be used not only in open-field cultivation but also in other cropping types should be developed.

Based on the results of this study, until the near future (approximately 2050), although climate change affects development in ‘Delaware’ grapes, the delay

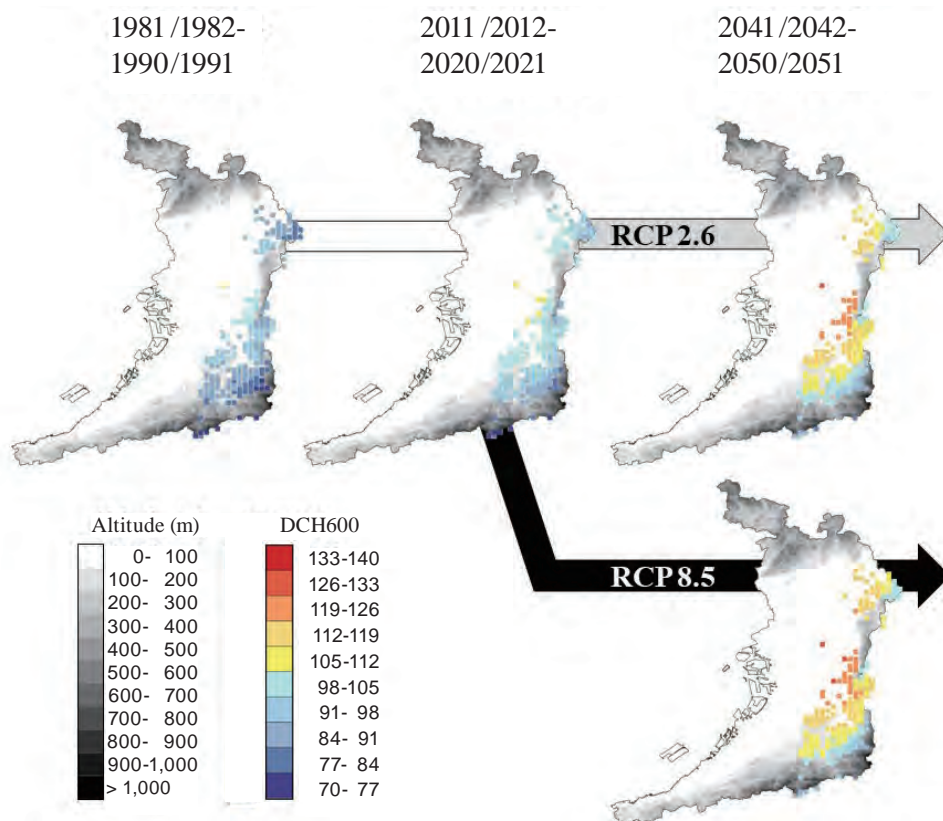
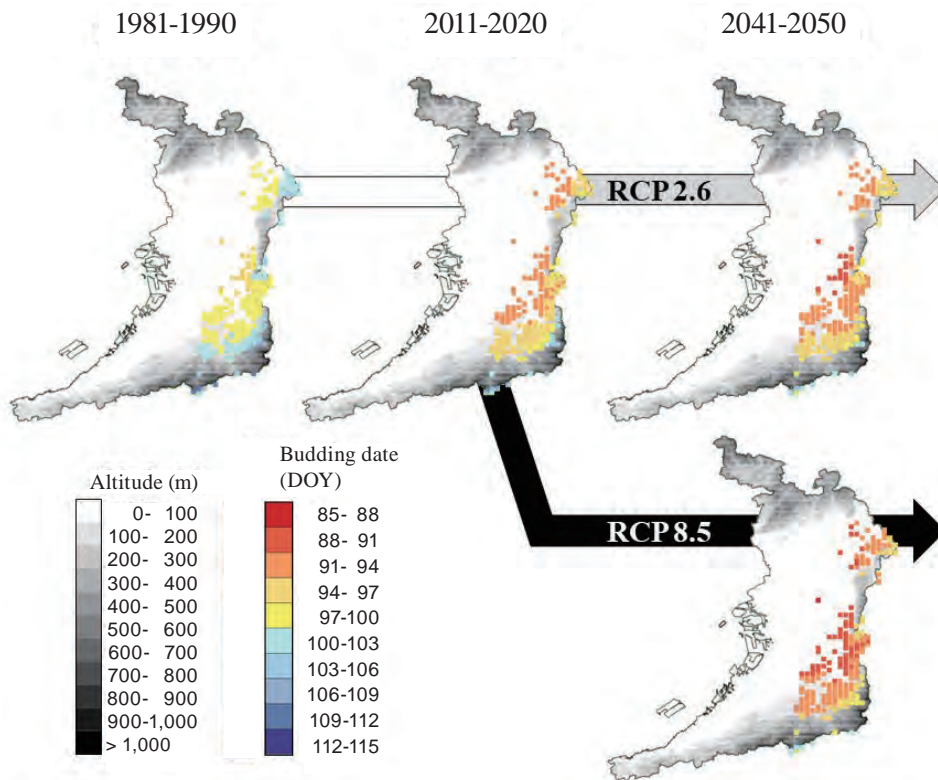
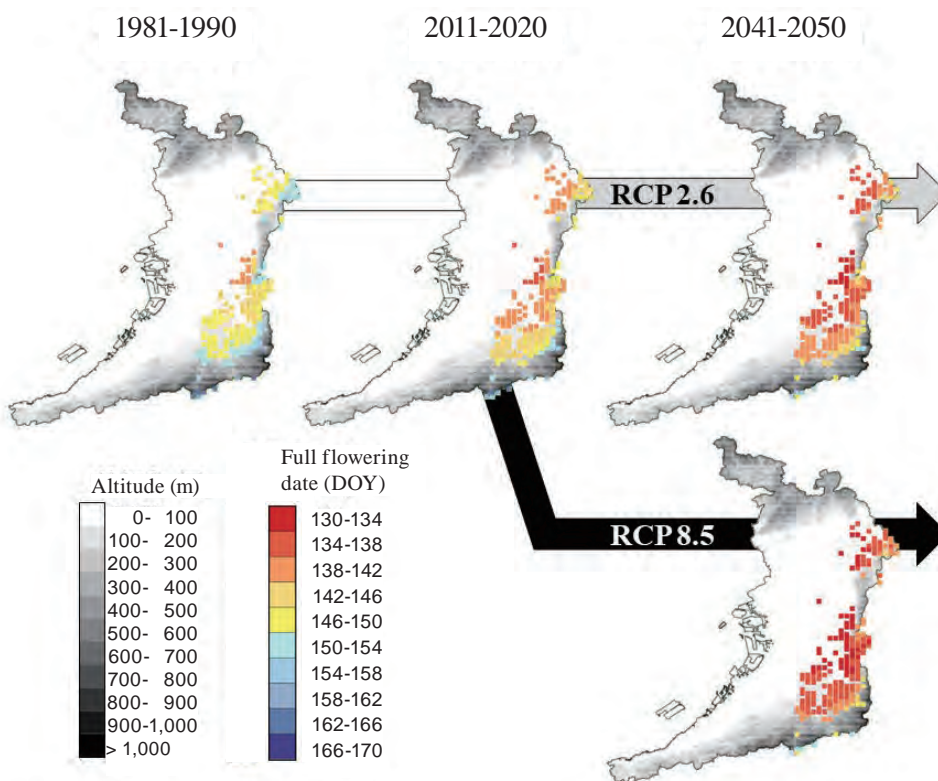


Fig. 7. Geographical distribution of the DCH600 of ‘Delaware’ grape in the major production area  
DCH600, the number of days from October 1





**Fig. 8. Geographical distribution of the budding dates of 'Delaware' grape in the major production area**  
DOY, the number of days from January 1



**Fig. 9. Geographical distribution of the full-flowering dates of 'Delaware' grape in the major production area**  
DOY, the number of days from January 1

for endodormancy breaking was 12-14 days in extent, and accelerations in budding and full-flowering were 1-3 days and 4-7 days in extent, respectively, based on those in 2011-2020 (present). Developmental changes to this extent can be handled by developmental prediction using crop developmental models and AMGSD, and the efficient use of existing treatments for endodormancy breaking. Thus, it is expected to sustain 'Delaware' grape production in Osaka until the near future by such advanced cultivation management. Furthermore, after 2050 under RCP2.6, air temperature seems to be stabilized, the impact on developmental change in 'Delaware' would also be similar to that around 2050. Hence, it may be possible to sustain 'Delaware' grape production by the same adaptation measures even after 2050. This suggests that 'Delaware' grape production in Osaka could be sustained by reducing greenhouse gas emissions. However, after 2050 under RCP8.5, a large delay in DCH600 and inadequate chilling were predicted, suggesting that changing cropping type or conversion to other fruit trees may be needed. As such future (2050-2100) predictions contain large uncertainties, it is important to prepare adaptation measures that can respond to a wide range of impact assessment results.

In Japan, the 2018 Climate Change Adaptation Act mandates prefectures and municipalities to form local climate change adaptation plans. By organizing the above adaptation measures by period, region, and climate change scenarios, we can prepare for the impact of future climate change on 'Delaware' grape production. In future studies, impact assessment of insect damage on 'Delaware' grape production that is expected to be affected by global warming, such as increases in pest generations and overwintering pests, will also need to be conducted in conjunction with analyses of the developmental changes.

## Acknowledgement

This research was funded by Osaka Prefectural Credit Federation of Agricultural Co-operatives.

## References

- Hirose, M. et al. (2000) Chilling requirement and chemical treatment for breaking dormancy in grapevines, peaches and Japanese pears. *Bulletin of the Oita Prefectural Agricultural Research Center*, **30**, 1-13 [In Japanese with English summary].
- Ishigooka, Y. et al. (2017) Large-scale evaluation of the effects of adaptation to climate change by shifting transplanting date on rice production and quality in Japan. *J. Agric. Meteorol.* **73**, 156-173.
- Kamimori, M. et al. (2019) Relationships between changes in air temperature and development of 'Delaware' grape for the past 48 years in Habikino, Osaka, Japan. *Hort. Res. (Japan)*, **18**, 133-138 [In Japanese with English summary].
- Kamimori, M. et al. (2020) Models for predicting dates of budding and full bloom of 'Delaware' grape based on the daily average temperature. *Hort. Res. (Japan)*, **19**, 175-181 [In Japanese with English summary].
- Kuroi, I. (1985) Effects of calcium cyanamide and cyanamide on bud break of 'Kyoho' grape. *J. Jpn. Soc. Hort. Sci.*, **51**, 301-306 [In Japanese with English summary].
- Magoon, C. A. & Dix, I. W. (1943) Observation on the response of grape vines to winter temperatures as related to their dormancy requirements. *Proc. Amer. Soc. Hort. Sci.*, **42**, 407-412.
- Matsumoto, N. et al. (2019) Effect of using rootstock low-chilling 'Okinawa' on 'Hikawahakuhou' peach flowering. *Hort. Res. (Japan)*, **18**, 7-16 [In Japanese with English summary].
- Ministry of Agriculture, Forestry and Fisheries (2021) Climate Change Adaptation Plan of MAFF. <https://www.maff.go.jp/j/kanbo/kankyo/seisaku/climate/adapt/attach/pdf/top-7.pdf>. Accessed on 1 December 2021 [In Japanese].
- Ministry of Agriculture, Forestry and Fisheries. (2018) Statistics of Agriculture, Forestry and Fisheries. [https://www.maff.go.jp/j/tokei/kouhyou/tokusan\\_kazyu/index.html](https://www.maff.go.jp/j/tokei/kouhyou/tokusan_kazyu/index.html). Accessed on 1 April 2021 [In Japanese].
- Mosedale, J. R. et al. (2016) Climate change impacts and adaptive strategies: lessons from the grapevine. *Global Chang Biol.*, **22**, 3814-3828.
- Nakagawa, H. & Horie, T. (1995) Modeling and prediction of developmental process in rice. *Jpn. J. Crop Sci.*, **64**, 33-42 [In Japanese with English summary].
- Nishimori, M. et al. (2019) SI-CAT 1 km-grid square regional climate projection scenario dataset for agricultural use (NARO2017). *J. Japan Soc. Sim. Tech.*, **38**, 150-154 [In Japanese].
- Ohno, H. et al. (2016) Development of grid square air temperature and precipitation data compiled from observed, forecasted, and climatic normal data. *Clim. Biosph.*, **16**, 71-79 [In Japanese with English summary].
- Osada, K. & Ohe, Y. (2010) Evaluating impacts of climate change on farm management -the case of grape farming in Yamanashi-. *J. Rural Probl.*, **46**, 266-269 [In Japanese with English summary].
- Seino, H. et al. (2016) An estimation of low temperature duration and high temperature duration from minimum and maximum temperature. *J. Agric. Meteorol.*, **37**, 123-126 [In Japanese].
- Sugiura, T. et al. (2009) Effects of global warming on fruit tree production and adaptation techniques. *Chikyu kankyo (Glob. Environ. Res.)*, **14**, 207-214 [In Japanese].
- Sugiura, T. et al. (2012) Overview of recent effects of global warming on agricultural production in Japan. *JARQ*, **46**, 7-13.
- Sugiura, T. et al. (2019) Assessment of deterioration in skin color of table grape berries due to climate change and effects of two adaptation measures. *J. Agric. Meteorol.*, **75**, 67-75.
- Togano, Y. et al. (2016) Effect of high temperature on budbreak of 'Delaware' grapevines. *Hort. Res. (Japan)*, **15**, 53-58 [In Japanese with English summary].